Developmental Biology 344 (2010) 658–668

Contents lists available at ScienceDirect

Developmental Biology

journal homepage: www.elsevier.com/developmentalbiology

Stabilization of ATF4 protein is required for the regulation of epithelial–mesenchymal transition of the avian neural crest

Takashi Suzuki, Noriko Osumi, Yoshio Wakamatsu *

Center for Translational and Advanced Animal Research on Human Diseases, Division of Developmental Neuroscience, Graduate School of Medicine, Tohoku University, Sendai, Miyagi 980-8575, Japan

ARTICLE INFO

Article history:
Received for publication 30 January 2010
Revised 13 May 2010
Accepted 16 May 2010
Available online 24 May 2010

Keywords:
Neural crest
EMT
ATF4
P300
Foxd3
Sox9

ABSTRACT

Epithelial–mesenchymal transition (EMT) permits neural crest cells to delaminate from the epithelial ectoderm and to migrate extensively in the embryonic environment. In this study, we have identified ATF4, a basic-leucine-zipper transcription factor, as one of the neural crest EMT regulators. Although *ATF4* alone was not sufficient to drive the formation of migratory neural crest cells, *ATF4* cooperated with *Sox9* to induce neural crest EMT by controlling the expression of cell–cell and cell–extracellular matrix adhesion molecules. This was likely, at least in part, by inducing the expression of *Foxd3*, which encodes another neural crest transcription factor. We also found that the ATF4 protein level was strictly regulated by proteasomal degradation and p300-mediated stabilization, allowing ATF4 protein to accumulate in the nuclei of neural crest cells undergoing EMT. Thus, our results emphasize the importance of the regulation of protein stability in the neural crest EMT.

Introduction

Epithelial–mesenchymal transition (EMT) is an important process in the tissue morphogenesis and organogenesis to generate motile cells (Acloque et al., 2009; Kalluri and Weeinberg, 2009 for reviews). During EMT, epithelial cells lose tight cell–cell adhesion, remodel their cytoskeleton so as to lose apicobasal polarity, degrade the basal membrane, and increase the association with the extracellular matrix. The neural crest is one of the model systems to study EMT in development. The neural crest is initially induced at the boundary of neural plate and non-neural ectoderm in vertebrate embryos by BMP and Wnt signalings (Kalcheim and Burstyn-Cohen, 2005; Sakai and Wakamatsu, 2005; Sauka-Spengler and Bronner-Fraser, 2008 for reviews), and crest cells subsequently undergo EMT. Highly motile crest cells eventually give rise to various tissues including neurons, glial cells, melanocytes, and cranial mesenchymal tissues in distinct locations (Le Douarin and Kalcheim, 1999).

In recent years, several transcription factors have been identified as important regulators of the neural crest EMT. Group E *Sox* genes such as *Sox8*, *9*, and *10*, which encode HMG-box transcription factors, appear to be important for formation of neural crest cells. In particular, *Sox9* seems to be essential for the regulation of EMT both in mouse and in chick (Cheung and Briscoe, 2003; Cheung et al., 2005; Sakai et al. 2006). Another EMT-related transcription factor gene, *Snail2*, is also essential for the neural crest EMT in avian embryos (Neito et al., 1994; Sakai et al, 2006), and Sox9 directly activates the transcription of *Snail2* (Sakai et al., 2006). *Foxd3*, a zinc-finger transcription factor gene, is also involved in the neural crest EMT phenotype (Dottori et al., 2001; Cheung et al., 2005). Thus, misexpression of *Foxd3* in the neural tube results in the induction of neural crest markers and in the reduction of *N-cadherin* and the induction of *Integrin-β1* (Cheung et al., 2005), but no (Kos et al., 2001; Suzuki et al., 2006) or limited (Dottori et al., 2001) induction of EMT was observed. Cotransfection experiments revealed that the combination of such transcription factors, *Sox9*, *Snail2*, and *Foxd3*, effectively induces ectopic EMT, along with other traits of neural crest cells, in the transfected neural tube (Cheung et al., 2005).

Posttranslational modifications of these transcription factors appear to be deeply involved in the neural crest development. For example, SOMOylation of *Xenopus* Sox9 modulates its function in neural crest induction and following differentiation (Taylor and LaBonne, 2006). Direct phosphorylation by PKA is essential for chick Sox9 to promote EMT, although this phosphorylation of Sox9 is not required for the activation of *Snail2* transcription (Sakai et al., 2006). Ubiquitination of *Xenopus* Snail2 by Ppa/Fbxl-14, one of the target-recognition subunits of Skp1-CDC53/Cullin-1-F-box protein (SCF) complex, limits the Snail2 protein level via proteasomal degradation (Vernon and LaBonne, 2006). Consistently, *Xenopus*

* Corresponding author. Center for Translational and Advanced Animal Research on Human Diseases, Division of Developmental Neuroscience, Graduate School of Medicine, Tohoku University, Sendai, Miyagi 980-8575, Japan. fax: +81 22 717 8205.
E-mail address: wakasama@mail.tains.tohoku.ac.jp (Y. Wakamatsu).

0012-1606/$ – see front matter © 2010 Elsevier Inc. All rights reserved.
doi:10.1016/j.ydbio.2010.05.492

Cullin-1 seems to be important for the allocation of the neural crest domain in the embryonic ectoderm (Voigt and Papalopulu, 2005).

In this study, we focus on the function of *Activation transcription factor 4* (*ATF4*, also known as *TAXCREB67*, *CREB-2*, *mTR67*, and *C/ATF*. See Ameri and Harris, 2008 for nomenclatures.), which appears to be expressed at high levels in the neural folds and the migrating neural crest cells of mouse embryos at least at the mRNA level (Murphy and Kolstø, 2000). *ATF4* gene encodes a basic-leucine-zipper-type transcription factor of the ATF/Creb family (Hai and Hartman, 2001, for a review). Numerous reports revealed the *ATF4* functions, such as modulation of metabolic and oxidative stress, regulations of eye development, hematopoiesis, bone morphogenesis, fertility, long-term memory storage, and synaptic plasticity (Ameri and Harris, 2008, for a review), but no function in neural crest development has been reported so far.

In this study, we have identified an avian homolog of *ATF4*, generated by an anti-ATF4 antibody, and found the ATF4 protein rapidly accumulates in the neural crest cells undergoing EMT. Subsequently, our gain- and loss-of-function experiments revealed that *ATF4* is one of the EMT regulating components of neural crest cells. We also show that the nuclear accumulation of ATF4 protein is facilitated in the neural crest cells undergoing EMT by p300-mediated stabilization.

Materials and methods

Experimental animals

Japanese quail (*Coturnix japonica*) eggs were obtained from Sendai Jun-ran, Sendai. Embryos were staged according to Hamburger and Hamilton (1951; HH stage).

In situ hybridization

Whole-mount and section *in situ* hybridizations were performed as described previously (Wakamatsu and Weston, 1997). The coding sequences of quail *ATF4* and *p300* were PCR-amplified from oligo (dT) primed E2 embryo cDNA pool, and were subcloned into *pBluescriptII* (Stratagene). The identity of avian *ATF4* cDNA was confirmed by an amino acid sequence comparison with CREB, ATF4, and ATF5 sequences of other species (see Supplemental Figure 1). The sequences of primers were as follows: ATF4F, GGAAGACACTGGTGATCTCC, ATF4R, CTACTCAGGGACTCTAGCTC; p300F, ATCCTCAGGCACAGCAGATG, p300R, CTAGTGTATGTCTAGTGTAC. Quail *Snail2*, *Sox2*, *Sox9*, and chicken *Sox10* cDNAs for cRNA probes were described previously (Cheng et al., 2000; Endo et al., 2002; Wakamatsu et al., 2004; Sakai et al., 2006). Chicken cDNAs of *Foxd3* (Kos et al., 2001), *Integrin-β1* (Cao et al., 2007), *N-cadherin* (Matsumata et al., 2005), *Cadherin7* and *Cadherin6B* (Nakagawa and Takeichi, 1995) were kind gift from Drs. C. Erickson, F. Gage, M. Uchikawa, and S. Nakagawa, respectively.

Antibodies and immunostaining

Anti-quail ATF4 polyclonal antiserum was raised by immunizing rabbits with a GST-tagged recombinant quail ATF4 protein (aa 1–296, ATF4$^{\Delta C}$). Thus, the corresponding *ATF4* sequence was inserted into *pET41a* (Novagen) for GST-fusion and bacterial expression. Recombinant GST-ATF4 fusion protein was purified from bacterial lysates with B-PER GST-fusion protein purification kit (Pierce). HNK1 mouse IgM and anti-Pax6 rabbit antibodies were described previously (Tucker et al., 1988; Inoue et al., 2000). PAX7 anti-Pax7, 3H11 anti-Laminin, and 6B3 anti-N-cadherin mouse IgG antibodies were obtained from Developmental Study Hybridoma Bank (University of Iowa). M2 anti-FLAG (mouse IgG1; Sigma), anti-GFP (rabbit polyclonal; Chemicon), 12CA5 anti-HA (mouse IgG; Roche), anti-ZO1 (rabbit polyclonal; Zymed), N15 anti-p300 (rabbit polyclonal; Santa Cruz), anti-phospho-Histone H3 (rabbit polyclonal; Upstate), and anti-active caspase 3 (rabbit monoclonal; BD Pharmingen) antibodies were commercially obtained. T8-754 anti-ZO1 mouse IgG was kindly provided by Dr. M. Furuse (Kitajiri et al., 2004). Fluorochrome-conjugated secondary antibodies were purchased from Jackson Immuno Research. Phalloidin conjugated with Texas Red-X or Oregon Green was obtained from Molecular Probes.

Immunological staining on sections and cultured cells was performed as described previously (Wakamatsu et al., 1993, 1997). Immunostaining for ATF4 and p300 required a short fixation condition (in 4% paraformaldehyde/PBS for 30 min at 4 °C). Sections treated with antibodies were also exposed to DAPI (Sigma) to visualize nuclei.

Expression vectors

PCR-amplified coding sequences of quail *ATF4* and *p300* were inserted into expression vectors *pyDF30* and *pyDF-HA* for N-terminal FLAG and HA tagging, respectively. Substitutions of β-TrCP1 binding site (aspartic acid 218 and serine 219) to alanine and the nuclear localization signal (lysine 281, 282, 284, 285; Cibeli et al., 1999) to asparagine were introduced to wild type *ATF4* sequence by using in vitro mutagenesis kit (Stratagene). For generating a repressor form of *ATF4* (*En-ATF4$^{\Delta N}$*), recombinant PCR was performed to generate N-terminal deletion of *ATF4* cDNA lacking the corresponding sequence (aa 1–180), and the deletion mutant cDNA was subsequently fused to the repression domain of *Engrailed2* (a gift from Dr. H. Nakamura; Matsunaga et al., 2000) to construct *pyDF-HA-En-ATF4$^{\Delta N}$*. The dominant-negative action of *En-ATF4$^{\Delta N}$* was confirmed by the fact that the transcriptional activation of *pCRE-luc*, a *Luciferase* reporter gene under the control of cAMP responsive element (Clontech), was activated by wild type *ATF4*, and that *En-ATF4$^{\Delta N}$* cotransfection attenuated the activation (Supplemental Figure 2). An expression vector of quail *Sox9* was previously described (Sakai et al., 2006). *GFP*-tagged chicken *Foxd3* expression construct (Kos et al., 2001) was kindly provided by C. Erickson, and GFP-tag was removed (*pyDF-HA-Foxd3*). Expression of these transgenes was confirmed by immunostaining of transfected cells by anti-epitope tag antibodies and/or Western blotting (data not shown). *pEGFP-N1* was purchased from Clontech. When HA-tagged *ATF4* was transfected into the neural tube along with *pEGFP-N1*, more than 70% of EGFP-positive cells coexpressed HA-ATF4 protein in their nuclei, revealed by immunostaining of sections. In contrast, only 17% of EGFP-positive cells coexpressed FLAG-tagged ATF4 protein, when cotransfected (see text and Fig. 6). Thus, for studying the misexpression phenotype, HA-tagged *ATF4* vector was used, while for testing the protein expression efficiency, FLAG-tagged versions were used. In addition, FLAG-tagged *ATF4* cDNAs were subcloned into *pCMS-EGFP* dual promoter vector (Clontech) to ensure coexpression of *EGFP* and *ATF4* transgenes in individual transfected cell.

Neural plate explant culture

Cultures of neural plate explants were performed as described previously (Wakamatsu et al., 2004, Sakai et al., 2005). In brief, intermediate fragments of the neural plate at the level of forebrain and midbrain were surgically dissected with a tungsten needle along with underlying mesoderm and endoderm. To remove the mesoderm and the endoderm, the dissected tissues were treated with Pancreatin (Wako). The isolated neural plates were cultured in F12-based medium containing 3% FCS on fibronectin (Sigma)-coated dishes. N2-supplement (1:100 dilution, Invitrogen) and recombinant human BMP4 (20 ng/ml; R&D Systems) were added in culture to induce neural crest formation. Ten micromolars of MG132 (Wako) was added in culture as a proteasome inhibitor, when indicated.

Electroporation-mediated gene transfer

Electroporations into the neural tube of E2 embryos and into the neural plate of stage 7 embryos for explant culture were performed as previously described (Funahashi et al., 1999; Wakamatsu et al., 2004; Sakai et al., 2005, 2006).

Whole-embryo culture in combination with electroporation was described previously (Endo et al., 2002, 2003, Sakai et al., 2005). In brief, before electroporation, the embryos adhering to collagen-coated membranes were set on a chamber with a 2-mm^2 positive electrode (Unique Medical Imada). A tungsten needle was used as the negative electrode. DNA solution (1.2 μl of 5 μg/μl in PBS containing 0.025% Fast Green) was placed on the right ectoderm of the embryo. The condition of electroporation was as follows: 7 V, 25 ms in duration, 200 ms interval, and three times. For cotransfection studies, *pEGFP-N1* and another expression vector were mixed at 1:1. For each experiment, 3 to 10 transfected embryos were examined, and only when at least two-thirds of examined embryos were similarly affected, the observed changes were identified as phenotypes.

Results

ATF4 protein rapidly accumulates in neural crest nuclei during EMT

First, we have examined *ATF4* mRNA expression in the early quail embryos by *in situ* hybridization. Tissue distribution of avian *ATF4* mRNA resembled that of the mouse homolog (Murphy and Kolstø, 2000), and elevated expression was confirmed in the neural folds, which overlapped with the expression of *Snail2* in premigratory crest cells (Figs. 1A, B, D, and E). *ATF4* expression was also detected in migrating cranial neural crest cells (Fig. 1C).

To observe ATF4 protein expression, polyclonal anti-ATF4 antibody was raised in a rabbit (see Materials and methods). At stage 8, before the EMT of cranial neural crest cells, ATF4 protein was detected in a fraction of Pax7-positive prospective neural crest cells (Figs. 2A, B, and I–K). At stage 8.5, when many crest cells were actively undergoing EMT, ATF4 protein accumulation in the nuclei was observed in many, if not all, the Pax7-positive crest cells (Figs. 2C and D). Interestingly, the neural tube cells, which did not accumulate ATF4 in their nuclei, weakly possessed anti-ATF4-immunoreactivity in their cytoplasm (Figs. 2L–N). At stage 9, migrating cranial crest cells expressed ATF4 protein (Figs. 2E and F). We also examined the ATF4 immunoreactivity at the trunk level of stage 12 embryos. Thus, ATF4 protein was highly accumulated in the emerging Pax7-positive crest cells on the top of the neural tube (Figs. 2G and H). Among non-crest tissues, we noticed that the epidermal ectoderm cells persistently expressed ATF4 protein at all stages and anteroposterior levels examined in this study (Figs. 2A and E, arrows).

To clarify the timing of ATF4 nuclear accumulation, we took advantage of neural plate explant culture system (Materials and methods; see also Wakamatsu et al., 2004; Sakai et al., 2005, 2006). Thus, culturing medial neural plate explants in the presence of BMP4 transformed the neural plate cells to neural crest fate. When cultured in this condition for 16 hours, many explant cells expressed neural crest markers (Sakai et al., 2005, 2006), and at the edge of the explants, many cells were undergoing EMT (Figs. 2O–W). These cells at the edge of the explant were losing cell–cell adhesion, visualized by the lack of ZO-1 immunoreactivity, and possessed high levels of ATF4 protein in their nuclei (Figs. 2R–W), while cells in the interior of the explant showed only weak and punctate staining for anti-ATF4 antibody in their cytoplasm (Figs. 2R–T). In 20-hour cultures, many crest cells with fibroblastic morphology and actin cytoskeleton dispersed, and the vast majority of these migrating crest cells were also ATF4-positive in their nuclei (approximately 95%; see Figs. 2X–Z). These observations indicated that ATF4 protein is rapidly accumulated in the nucleus at the onset of crest EMT.

ATF4 participates in the regulatory program of the neural crest EMT

Misexpression of ATF4 in the neural tube induces partial EMT phenotype

To examine possible roles of neural crest transcription factors in vivo, transfection of expression vectors into the neural tube of E2 avian embryos has often been practiced (Dottori et al., 2001; Kos et al., 2001; Cheung and Briscoe, 2003; Wakamatsu et al., 2004; Cheung et al., 2005; McKeown et al., 2005; Suzuki et al., 2006). We thus performed unilateral cotransfection of *EGFP* and HA-tagged *ATF4* expression vectors and observed the phenotype 6, 12, and 24 hours later (Figs. 3 and 4). The nuclear localization of HA–ATF4 protein was confirmed by anti-HA immunostaining (data not shown). At 6 hours, the morphology of the *ATF4*-transfected neural tube was grossly normal compared to the *EGFP*-transfected control neural tube (Fig. 3A). Many transfected cells showed apicobasally elongated shape (Fig. 3A), although actin cytoskeleton of neuroepithelial cells seemed to be slightly irregular in *ATF4*-transfected neural tube (Fig. 3A). At 12 and 24 hours, the *ATF4*-transfected neural tubes became thinner compared to the contralateral side of the same embryo or compared to control neural tubes transfected with *EGFP* (Fig. 3A). While cells in *EGFP*-transfected neural tube remained apicobasally polarized, many *ATF4*-transfected cells rounded and fell off into the lumen of the neural tube (Fig. 3A).

Although we could detect many phospho-Histone H3 (pH3)-positive mitotic figures at all stages examined, suggesting that *ATF4*-transfected cells could proliferate, these mitotic cells often failed to align along the apical side of the neural tube (Fig. 3B). Thus, while the proportion of such abventricular pH3-positive cells in *EGFP*-transfected neural tubes was 1.3% (2/150 cells, $n=3$) 24 hours after transfection, that in *EGFP*/*ATF4*-cotransfected neural tubes was 20.5% (41/200 cells, $n=3$). There was also an increase of active caspase 3-positive apoptotic cells (Fig. 3B). Thus, while the proportion of active caspase 3/EGFP double-positive cells among EGFP-positive cells in *EGFP*-transfected neural tubes was

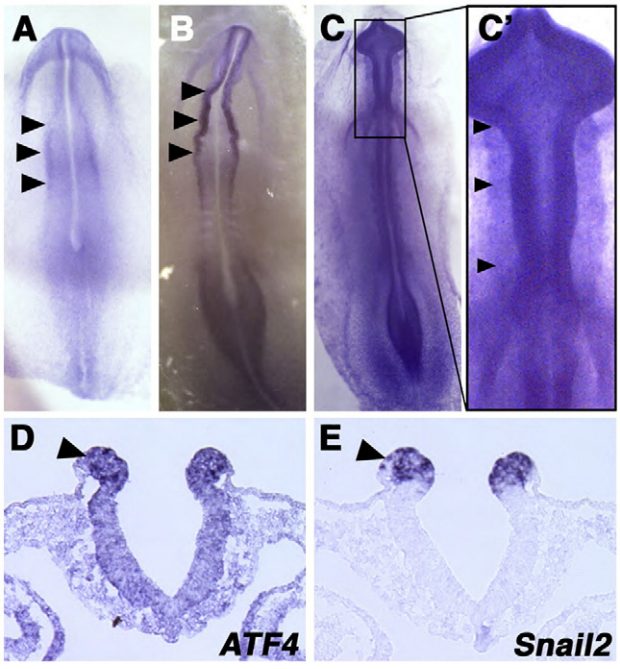

Fig. 1. Expression of *ATF4* mRNA in the cranial neural crest. Whole-mount dorsal view of HH stage 7, 8, 9 quail embryos (A–C), and neighboring transverse sections of stage 8 embryo (D and E). An elevation of *ATF4* expression is observed in the neural folds (A and B, arrowheads). *ATF4* mRNA is also detected in migrating cranial crest cells (C′, arrowheads). Higher expression of *ATF4* is observed in the neural crest cells (D, arrowhead), which are positive for *Snail2* (E, arrowhead).

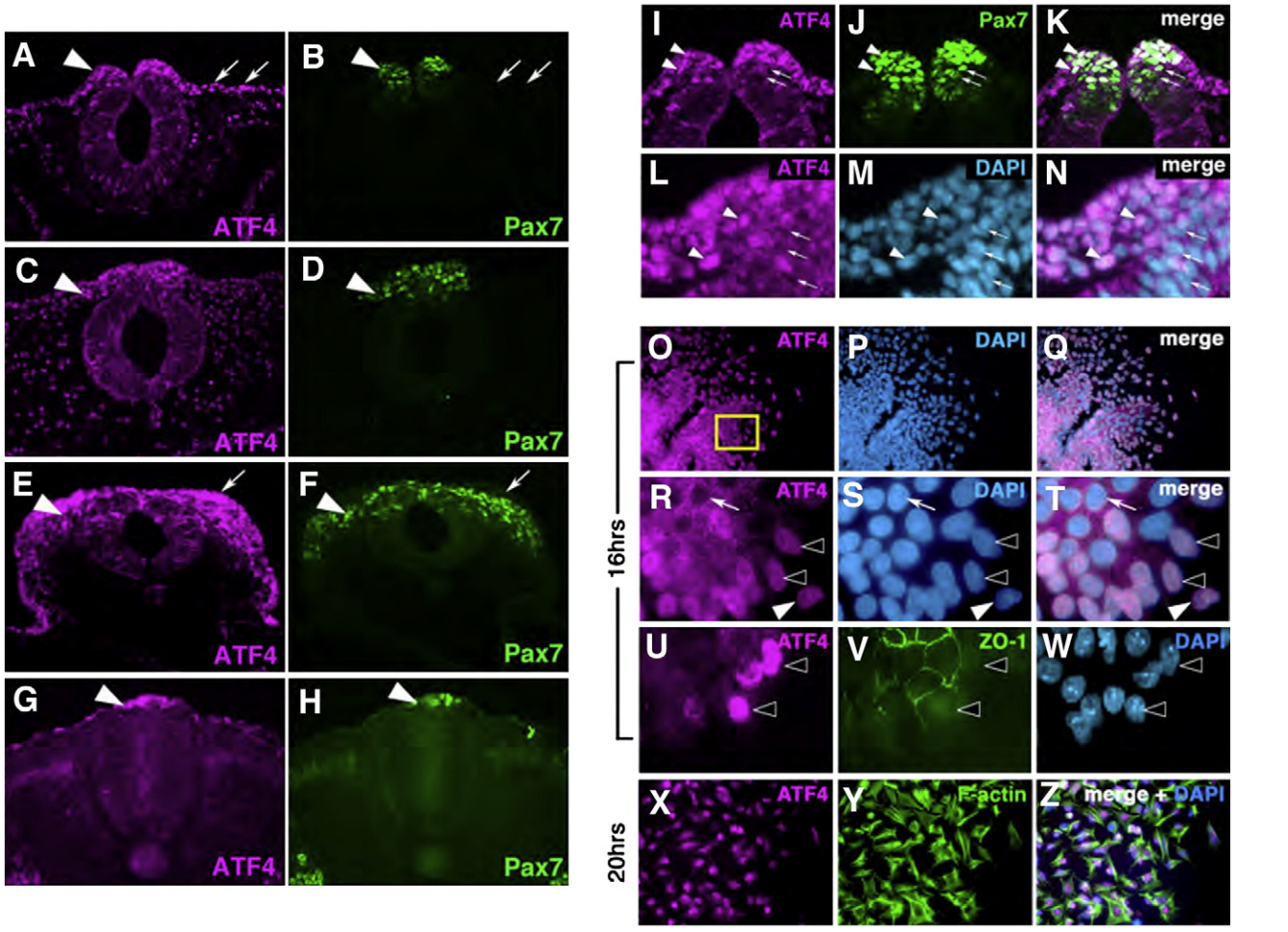

Fig. 2. Expression and cellular localization of ATF4 protein in the neural crest cells. Transverse sections of HH stage 8 (A and B), 9 (C and D), 11 (E and F), and 14 (G and H) were double-stained with anti-ATF4 and anti-Pax7 antibodies. High levels of ATF4 protein expression are observed in Pax7-positive premigratory and migrating neural crest cells (arrowheads). Higher magnification of A and B (I–K) reveals that some Pax7-positive cells coexpress ATF4 (arrowheads), while others are ATF4-negative (arrows). Higher magnification of C and D (L–N) reveals that migrating crest cells possess ATF4 protein in their nuclei (arrowheads), but many cells remaining in the neural tube have weak, cytoplasmic anti-ATF4 immunoreactivity (arrows). DAPI indicates nuclei. (O–Z) Neural plate explants were cultured in the presence of BMP4. R–T show higher magnification views corresponding to the area indicated in O. At 16 hours of culture (O–W), ATF4 is highly accumulated in the nuclei of cells residing at the edge of the explant after (white arrowhead) or undergoing (black arrowheads) EMT, while interior cells possess weak anti-ATF4 immunoreactivity in their cytoplasm (arrow) (R–T). U–W show a high-magnification view of the edge of a similar explant, stained with anti-ATF4, anti-ZO-1, and DAPI. Cells losing cell–cell junction accumulates ATF4 protein in their nuclei (arrowheads). At 20 hours of culture, dispersing crest cells are ATF4-positive in their nuclei (X–Y). Phalloidin staining of F-actin reveals mesenchymal cell morphology (Y).

0.5% (8/1514 cells, $n=3$) 24 hours after transfection, that in *EGFP*/*ATF4*-cotransfected neural tubes was 5.6% (99/1760 cells, $n=3$). Consistent with the fact that no *ATF4*-transfected cells came out from the ectopic position of the neural tube, basement membrane appeared to be intact (Fig. 3B), although *ATF4*-transfected neural tube cells sometimes possessed Laminin ectopically suggesting that the transfected neural tube cells failed to exclusively target deposition of Laminin protein to the basal surface. Thus, the thinning of the neural tube by *ATF4* misexpression seemed to be caused by the combination of cell shape change, probably by losing epithelial polarity, cell death, and detachment of cells into the lumen.

The detachment of cells from their apical junctional sites at the lumen suggested that the transfected neural tube cells might have lost cell–cell adhesion. Thus, expression of cell–cell and cell–ECM adhesion molecules was also examined. It has been known that the *cadherin* subtype changes from *N-cadherin* to *Cadherin6B* during crest induction, and migrating crest cells further downregulate *Cadherin6B* and begin to express *Cadherin7* in avian embryos (Nakagawa and Takeichi, 1995). While no change in the expression of N-cadherin protein was observed at 6–hours after *ATF4*-transfection (Figs. 4A and B), at 12 and 24 hours, the expression of N-cadherin was clearly decreased (Figs. 4F, G, K, and L). Consistent with the reduction of *N-cadherin* expression, *ATF4* transfection also downregulated the expression of *Sox2* (Figs. 4H and M), an activator of *N-cadherin* transcription (Matsumata et al., 2005) and an inhibitor of neural crest formation (Wakamatsu et al., 2004). We also observed *Cadherin6B* mRNA expression in the pre-EMT crest cells being diminished by *ATF4* misexpression (Figs. 4P and Q). In the *ATF4*- transfected neural tube, we not only observed downregulation of genes indicated above but also detected ectopic inductions of *Cadherin7*, and *Integrin-β1*, which is normally expressed in migrating crest cells as a receptor for the ECM binding (Duband et al., 1991), at all stages examined (Figs. 4D, E, I, J, N, and O).

As indicated above, before the neural crest EMT, ATF4 protein localized in the cytoplasm at low levels, and subsequently accumulated in the nuclei during EMT. To ensure the observed phenotypes caused by *ATF4* misexpression in the neural tube as the effect of ATF4 protein in the nuclei, an expression vector carrying *HA-ATF4* with mutations in the nuclear localization signal (*HA-ATF4*$^{\Delta NLS}$) was constructed according to Cibeli et al., 1999 (see also Materials and methods). The cytoplasmic accumulation of HA-ATF4$^{\Delta NLS}$ protein was clearly observed when transfected into the neural tube (Supplemental Figure 3A), and neither morphological changes of the neural tube nor a reduction of N-cadherin expression was observed (Supplemental Figure 3B).

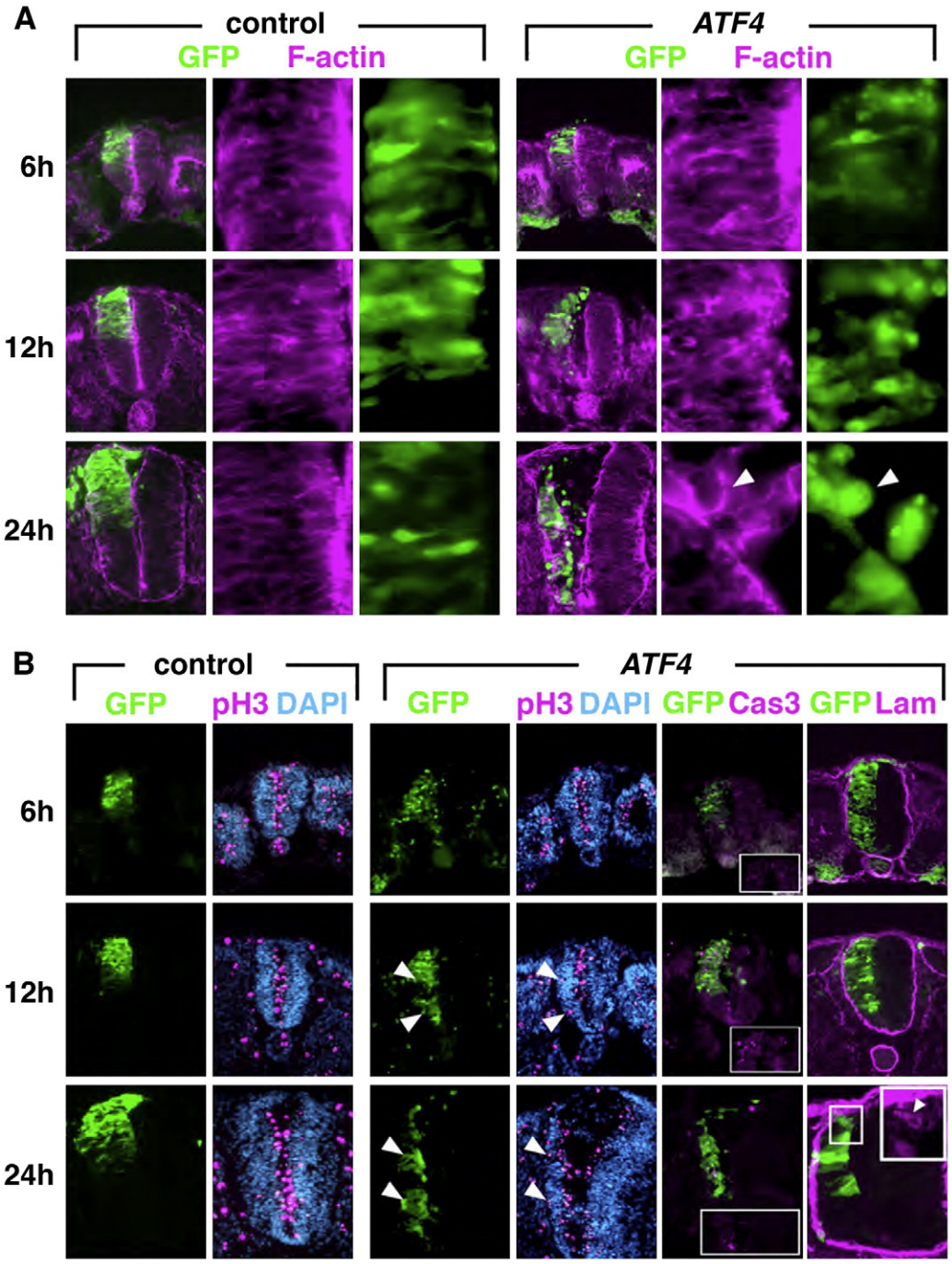

Fig. 3. Structural changes of *ATF4*-transfected trunk neural tube. (A) morphological changes of neural tubes and neuroepithelial cells by cotransfection of *EGFP* and *HA-ATF4* misexpression, 6, 12, and 24 hours after electroporation. Compared to the *EGFP*-transfected control, *ATF4* misexpression gradually causes degradation of the neural tube (left columns). High-magnification views (middle and right columns) reveal that *ATF4*-transfected cells lose apicobasally elongated cell shape (see controls) and show round morphology. Many transfected (arrowheads) and untransfected cells are found in the lumen of the neural tube 24 hours after *ATF4*-transfection. (B) Distribution of phospho-Histone H3 (pH3)-positive mitotic cells, active caspase 3 (Cas3)-positive dying cells, and the basement membrane. While mitotic cells align along the apical lumen of the neural tube in the control samples, at 12 and 24 hours after *ATF4* transfection, transfected neural tubes possess mitotic cells in ectopic position (arrowheads). Cas3-positive cells are increased on the transfected side (insets indicate the dorsal neural tube area) 12 and 24 hours after transfection. Anti-Laminin staining shows that, while *ATF4* misexpression does not disrupt basement membrane, ectopic deposition of Laminin is observed in the neural tube (higher magnification in the inset).

These phenotypes obtained by misexpression of *ATF4* indicated that *ATF4* might participate in neural crest EMT, but because transfected cells failed to disrupt basement membrane and no expression of neural crest marker HNK1 epitope was induced (Figs. 4C and R), *ATF4* transfection did not seem to be sufficient for neural tube cells to acquire full neural crest identity. In fact, *ATF4* misexpression rather reduced the basal level expression of HNK1 epitope in the neural tube (Fig. 4R).

ATF4 function is required for the neural crest EMT and the following dispersal

Next, we examined the requirement of *ATF4* in the neural crest EMT. Although an elevated expression of *ATF4* mRNA was observed in the neural folds of mouse embryos (Murphy and Kolstø, 2000), no noticeable phenotype has been reported in the neural crest of *ATF4*-null mice (Tanaka et al., 1998; Hettman et al., 2000; Masuoka and Townes, 2002; Yang and Karsenty, 2004), suggesting that there might be functionally

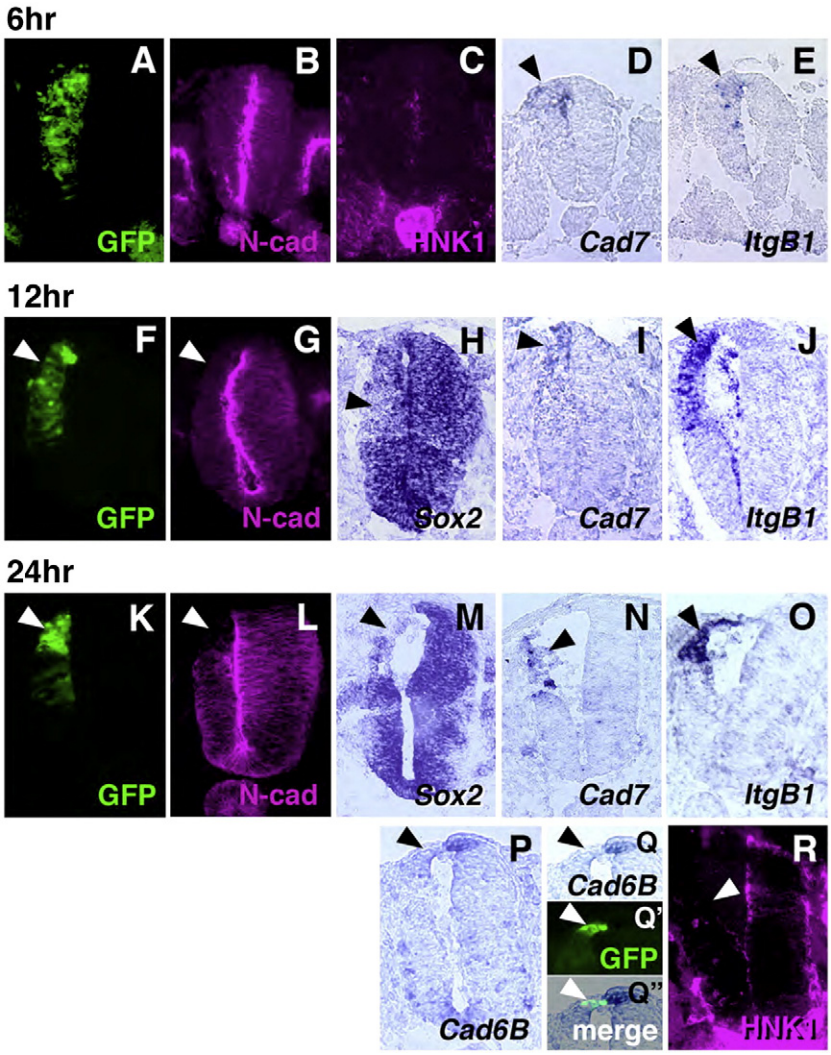

Fig. 4. Effects of *ATF4* misexpression on expression of adhesion molecules in the trunk neural tube. Cotransfection of *EGFP* and HA-tagged *ATF4* expression vectors. *ATF4*-transfected cells does not show changes in N-cadherin protein (N-cad) expression 6 hours after electroporation (A and B), clear downregulation is observed 12 and 24 hours after transfection (F, G, K, and L). Coincidently, expression of *Sox2*, an activator of *N-cadherin* transcription, is repressed (H and M). While *ATF4* misexpression upregulates expression of *Cadherin7* (*Cad7*; D, I, and N) and *Integrin-β1* (*ItgB1*; E, J, and O), it downregulates *Cadherin6B* (*Cad6B*) expression (P and Q). Q, Q′, Q″ reveal downregulation of *Cad6B* in EGFP-positive *ATF4*-transfected cells. ATF4 transfection does not induce HNK1 epitope expression (C and R) and rather represses basal expression of HNK1 (arrowhead in R) seen on the contralateral side.

redundant genes. We therefore took advantage of a dominant-negative approach to interfere the function of endogenous *ATF4*. Thus, the N-terminal transcriptional activation domain of ATF4 (Schoch et al., 2001) was replaced with the repressor domain of Engrailed (En-ATF4$^{\Delta N}$, see Fig. 5A). The dominant-negative effect of *En-ATF4*$^{\Delta N}$ over wild type was confirmed by Luciferase assay with *pCRE-luc* reporter construct (Supplemental Fig. 2, see also Materials and methods).

To observe the effect of *En-ATF4*$^{\Delta N}$ transfection in vivo, this construct was coelectroporated into the cranial neural folds of stage 6 embryos along with the *EGFP* expression vector. The transfected embryos were allowed to develop for an additional 16 hours, and the distribution of neural crest cells was assessed by the expression of *Sox10* (Figs. 5B–I). *Sox10*-positive neural crest cells were well dispersed and reached to the prospective cranial anlagen, when transfected only with *EGFP* (Figs. 5B–E). In contrast, *En-ATF4*$^{\Delta N}$-transfected crest cells could not efficiently disperse (Figs. 5F–I). This could have suggested that *En-ATF4*$^{\Delta N}$ cell-autonomously interfered the crest migration by altering the expression of cell–cell and cell–ECM adhesion molecules, indicated by the misexpression studies shown above. Alternatively, however, the transfection into the epidermal ectoderm could have changed the migration pathway environment by interfering ATF4 function in the epidermis.

To exclude an indirect effect on EMT and migration and to observe cellular changes by *En-ATF4*$^{\Delta N}$ transfection, neural plate explants were cotransfected with expression vectors of *En-ATF4*$^{\Delta N}$ and *EGFP*, and neural crest fate was induced by BMP4 treatment (Figs. 5J–W). Explants were cultured for 20 hours, which was long enough to detect many neural crest cells showing fibroblastic morphology and dispersing on the culture dish after EMT (Figs. 5L–N). When *En-ATF4*$^{\Delta N}$ was transfected, more than 50% of well-transfected explants failed to adhere to the culture dish (Figs. 5J and K), suggesting a low affinity to ECM and a tight cell–cell adhesion. In the *En-ATF4*$^{\Delta N}$-transfected explants successfully adhered to the culture dish, the transfected cells tended to form aggregates and failed to disperse (Figs. 5O–Q). While the *EGFP*-transfected cells possessed fragmented anti-ZO-1 staining (Figs. 5R–T), the *En-ATF4*$^{\Delta N}$–transfected cells often retained junctional complex, as revealed by anti-ZO-1 immunoreactive meshwork (Figs. 5U–W, see also Fig. 5X for a measurement).

ATF4 promotes neural crest EMT in concert with other transcription factors

A previous report revealed that combinatorial transfection of transcription factor genes efficiently promote ectopic EMT of neural tube cells, suggesting that the neural crest EMT may require a set of

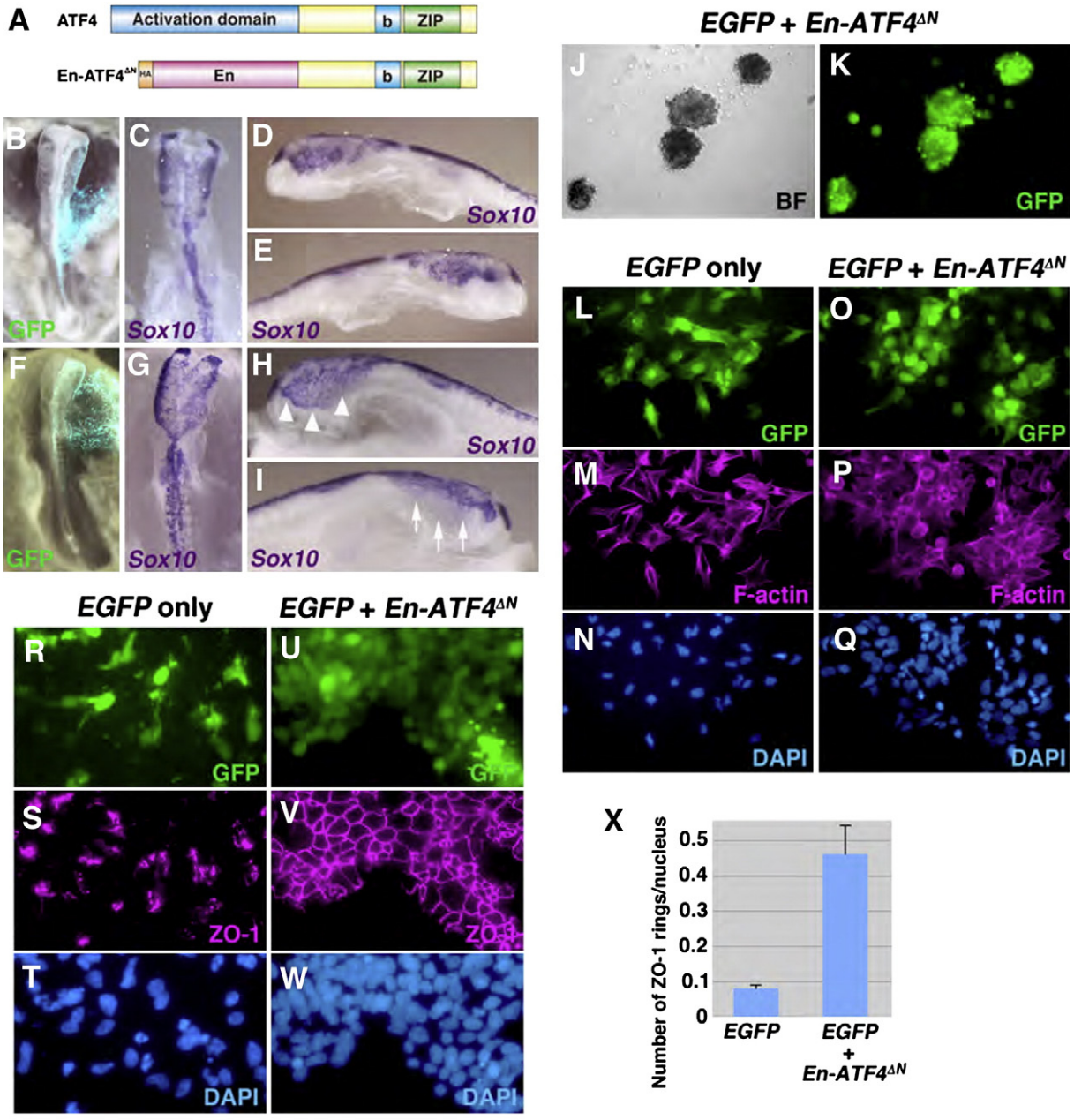

Fig. 5. Dominant-negative *ATF4* affects neural crest EMT and migration. (A) Structure of dominant-negative ATF4. N-terminal activation domain is replaced with Englailed2 repressor domain (En). HA-tag is also added N-terminally. (B–I) Whole-mount preparations of embryos transfected with *EGFP* alone (B–E) or cotransfected with *EGFP* and *En-ATF4*$^{\Delta N}$ (F–I) into the ectoderm including the neural crest cells before the migration. While transfection of *EGFP* alone does not affect the distribution of *Sox10*-expressing cranial crest cells, *Sox10*-positive crest cells fail to migrate effectively in the *En-ATF4*$^{\Delta N}$-transfected embryo (arrows in I), compared to the untransfected side (arrowheads in H). (J and K) BMP4-treated *En-ATF4*$^{\Delta N}$-transfected neural plate explants that failed to adhere to the culture dish. BF: bright field. (L–Q) BMP4-treated neural plate explants stained with phalloidin for F-actin and DAPI for nuclei. While *EGFP*-transfected explant cells show fibroblastic morphology and disperse on the culture dish (L–N), similar cells cotransfected with *EGFP* and *En-ATF4*$^{\Delta N}$ fail to disperse and form aggregates (O–Q). (R–W) BMP4-treated explants stained with anti-ZO-1 antibody for cell–cell junction and DAPI for nuclei. While explant cells transfected with *EGFP* show fragmented ZO-1 immunoreactivity (R–T), *En-ATF4*$^{\Delta N}$-transfected explant cells retain meshwork-like cell–cell junction (U–W). (X) Counting ZO-1-stained rings/nucleus. The number of ZO-1 ring was divided by the number of nuclei. More than 10 explants, more than 5000 cells were counted to obtain each value. Error bars indicate standard deviations. Note: because the majority of *En-ATF4*$^{\Delta N}$-transfected explant cells form large cell aggregates, which makes cell count extremely difficult, only portions of the explants showing monolayers (see U–W) were subjected for counting. Thus, the obtained value of *En-ATF4*$^{\Delta N}$-transfected explants is likely an underestimation.

the activities of crest transcription factors (Cheung et al., 2005; see also reviews mentioned above). Thus, misexpression of any single transcription factor appeared to be insufficient to induce "immediate" EMT from the transfected neural tube in vivo, while simultaneous cotransfection of a few was more effective (Cheung et al., 2005).

Because the phenotypes of *ATF4* misexpression resembled that of *Foxd3*, namely the repression of *N-cadherin*, the induction of *Integrin-β1*, and mislocalization of Laminin protein (see Cheung et al., 2005), as well as the repression of *Cadherin6B* (data not shown), we hypothesized that the cotransfection of *Sox9* and *ATF4*, instead of *Foxd3*, would effectively promote ectopic EMT. As a result, 24 hours after transfection, the basal lamina was extensively disrupted, and many transfected neural tube cells became HNK-1-positive and migrated out of the neural tube, compared to the transfection of *ATF4* or *Sox9* alone (Figs. 6A–I).

Our observations indicated above suggested an epistatic relationship between *ATF4* and *Foxd3*. Misexpression of *Foxd3* failed to induce *ATF4* (Figs. 6M and N), although it induced *Sox10* as reported

previously (data not shown, but see Cheung and Briscoe, 2003). In contrast, *ATF4* misexpression induced *Foxd3* in the transfected neural tube (Figs. 6K–L). These results indicated that *ATF4* would be epistatically upstream of *Foxd3*. *ATF4* transfection did not affect the endogenous expression of *Sox9*, *Sox10*, *Snail2*, *Pax7*, and *Pax6* (data not shown), indicating that *ATF4* misexpression would affect neither the neural crest induction nor the neural tube patterning.

Stability control is important for the neural crest-restricted rapid elevation of ATF4 protein

Previous reports have indicated the importance of the stability control of ATF4 protein in cultured cell lines (Lassot et al., 2001). In fact, we have found that ATF4 protein weakly localized in the cytoplasm of neural epithelial cells, and that, during the EMT, not only ATF4 proteins accumulated in the nucleus, but also the protein levels seemed significantly upregulated. In contrast, *ATF4* mRNA expression appeared to be relatively broad in the developing neural tube, and a graded upregulation toward the dorsal neural folds was observed. These data suggested the existence of posttranscriptional regulation of ATF4 protein expression in the neural epithelium and the neural crest.

β-TrCP1, a ligand-binding subunit of $SCF^{\beta\text{-TrCP}}$ E3 ubiquitin ligase complex, was shown to downregulate ATF4 protein expression by ubiquitination leading to proteasomal degradation (Lassot et al., 2001). To test if ATF4 protein level is regulated in avian neural crest, neural plate explants were treated with MG132, a proteasome inhibitor, and an increase of anti-ATF4 immunoreactivity was observed (Fig. 7A). Next, we constructed an expression vector of FLAG-tagged *ATF4* with mutations in the β-TrCP1 binding sequence (*ATF4* $^{D217A/S218A}$. see also Materials and methods). *EGFP* expression vector was cotransfected either with FLAG-tagged wild type *ATF4* or *ATF4* $^{D217A/S218A}$ mutant into the neural tube, and expression efficiency was examined 16 hours after transfection (Figs. 7B and C). While many EGFP-positive, FLAG-negative cells were detected when wild type *ATF4* was transfected, a drastic increase of EGFP/FLAG-double-positive cells was observed when *ATF4* $^{D217A/S218A}$ was transfected. These results were further confirmed by the use of dual promoter vector (see Materials and methods), which ensured coexpression of *EGFP* and *FLAG-ATF4* (Fig. 7D). *FLAG-ATF4* $^{D217A/S218A}$ seemed to be fully active as transfected neural tubes showed a severe reduction of N-cadherin expression and the neural tube degradation 24 hours after transfection (Fig. 7E).

In a previous report, it was shown that p300 Histone acetyl-transferase binds to the N-terminal region of ATF4 protein and protects it from the β-TrCP-mediated degradation in HeLa and 293 T cell lines (Lassot et al., 2005). Thus, we first examined the expression of *p300* mRNA by *in situ* hybridization. *p300* mRNA appeared to be ubiquitously expressed in the early avian embryo, and no elevation was found in the *Snail2*-positive neural crest cells (Figs. 8A and B). However, p300 protein was highly accumulated in the nuclei of neural crest cells, while fewer p300-positive cells were found in the rest of the neural tube, and this protein distribution was similar to that of ATF4 (Figs. 8C and D; see also above). Accordingly, to test if β-TrCP-mediated degradation would contribute to the low levels of ATF4 protein expression in the neural tube, a *p300* expression vector was transfected into the neural tube. As a result, an ectopic upregulation of endogenous ATF4 protein expression was detected in the neural tube (Figs. 8E–G). These observations suggest that endogenous p300 protein might indeed stabilize ATF4 protein in the neural crest cells undergoing EMT.

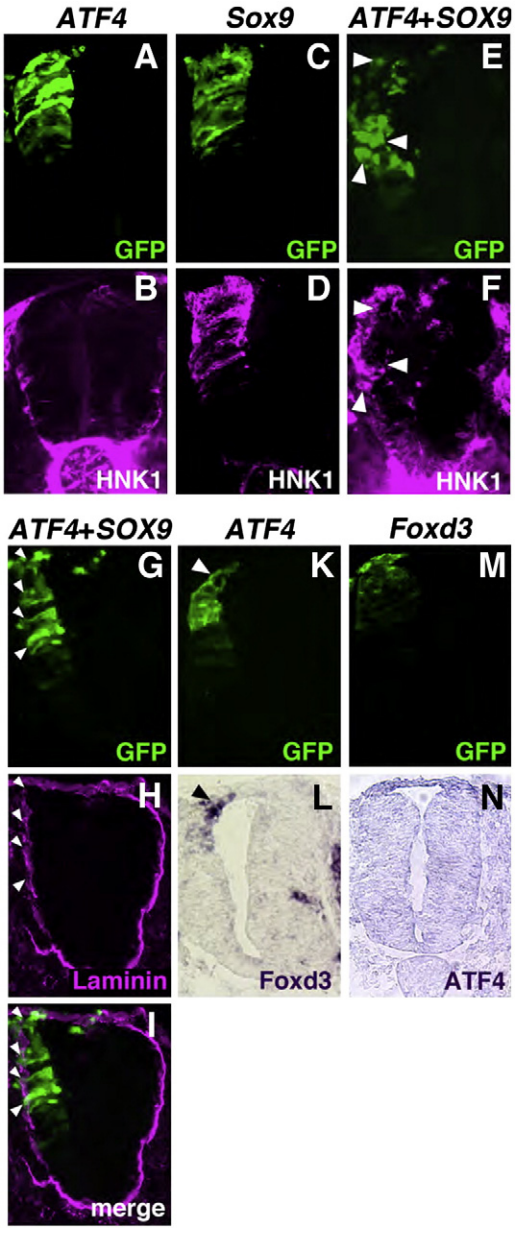

Fig. 6. Relationship of *ATF4* and other neural crest transcription factors. While transfection of *ATF4* or *Sox9* does not results in ectopic EMT of transfected neural tube cells in 24 hours (A–D), cotransfection of *ATF4* and *Sox9* results in a degradation of the neural tube (G and H) and the disruption of the basal lamina (E and F), leading to the delamination of transfected HNK-1-positive cells (E and F). Sox9 transfection induces HNK-1 expression (C and D). (K–N) While *Foxd3*-transfection does not affect the expression of *ATF4* mRNA (M and N), *ATF4*-misexpression induces ectopic expression of *Foxd3* (K and L).

Discussion

ATF4, a new neural crest-related transcription factor

In this study, we have shown that *ATF4* expression is upregulated in neural crest cells and that ATF4 protein rapidly accumulates in the nucleus during EMT, suggesting the involvement of *ATF4* in the control of neural crest EMT. Consistently, both misexpression and dominant-negative expression studies indicated that *ATF4* functions for the promotion of crest EMT by regulating the expression of cell–cell and cell–ECM adhesion molecules. Such functions of *ATF4* can be attributed to the transcriptional activation of downstream targets, because *ATF4*$^{\Delta NLS}$ showed no obvious phenotype when transfected into the neural tube. While misexpression of group E *Sox* genes, such as *Sox9* and *Sox10* takes 1.5–2 days for induction of ectopic EMT in the neural tube (Cheung and Briscoe, 2003; Mckeown et al., 2005), cotransfection of *Sox9*, *Snail2*, and *Foxd3* (Cheung et al., 2005) or the

combination of *Sox9* and *ATF4* (this study) efficiently induces ectopic EMT from the neural tube in 24 hours. Our results therefore indicate that *ATF4* can substitute for *Foxd3*, likely by promoting *Foxd3* expression. These results are also in agreement with the relatively late expression of both ATF4 protein (see above) and *Foxd3* mRNA (Sakai et al., 2006) in the crest cells undergoing EMT. It remains to be

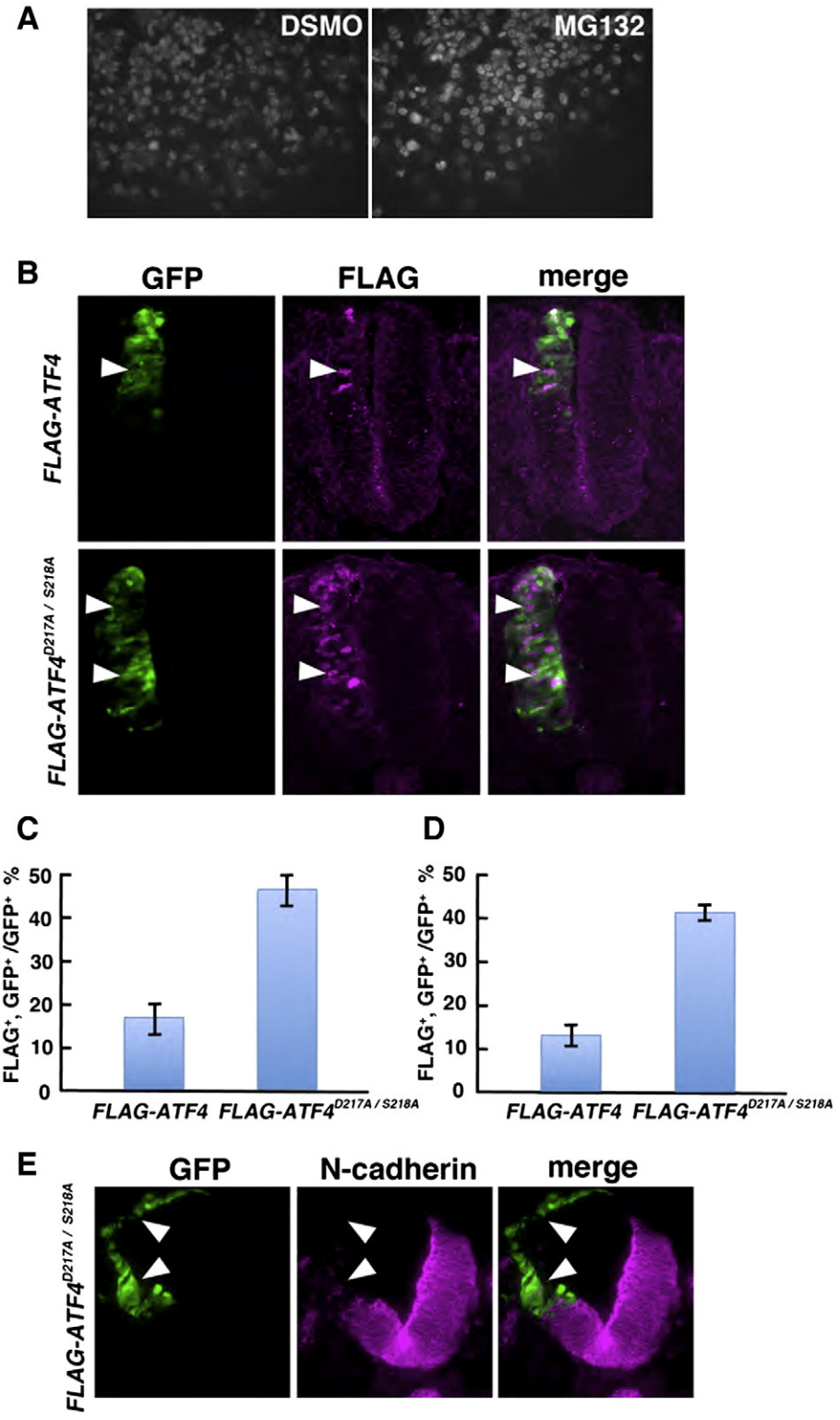

Fig. 7. Proteasomal degradation limits the level of ATF4 protein expression in the neural tube and neural crest. (A) Proteasome inhibitor (MG132)-treated neural plate explant cells express higher levels of ATF4 protein, compared to the explant cells treated with DMSO, the vehicle of MG132. (B) Expression of exogenous, FLAG-tagged ATF4 proteins in the neural tube. Expression vectors of FLAG-tagged wild type *ATF4* or *ATF4* carrying mutations in the β-TrCP1 binding site (*FLAG-ATF4D217/S218A*) are cotransfected with *EGFP* into the neural tube, and expression of exogenous ATF4 protein expression is detected by anti-FLAG antibody 16 hours after transfection. (C) Cell counts of (B). Expression of FLAG-ATF4D217/S218A protein is nearly three times as effective as the wild type ATF4. (D) Cell counts using dual promoter vector *pCMS-EGFP*, ensuring coexpression of *EGFP* and *FLAG-ATF4*. More than 500 EGFP-positive cells were examined in each embryo, and averaged proportions of FLAG–EGFP double-positive cells among EGFP-positive cells taken from three embryos are indicated for C and D. Error bars indicate standard deviation. (E) Misexpression of *FLAG-ATF4D217/S218A* causes a clear repression of N-cadherin expression and severe neural tube thinning (arrowheads) 24 hours after transfection.

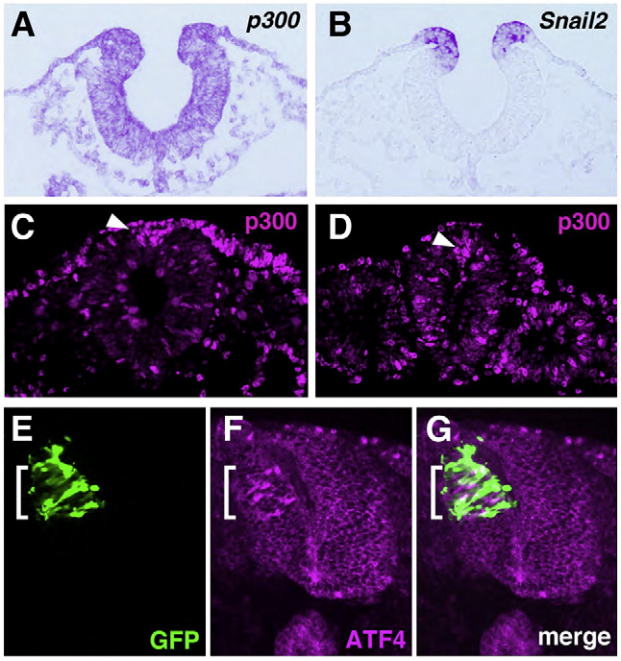

Fig. 8. Expression and transfection of *p300*. (A and B) Transverse sections of stage 8 embryo. While *Snail2* expression is highly restricted in the neural crest cells (B), *p300* mRNA expression shows ubiquitous distribution (A). (C and D) Immunostaining reveals restricted expression of p300 protein. p300-immunoreactivity is particularly high in the premigratory neural crest cells at the hindbrain level of stage 9 embryo (arrowhead in C), and at the trunk level of stage 11 embryo (arrowhead in D). (E–G) Misexpression of *p300* along with *EGFP* shows ectopic accumulation of endogenous ATF4 protein in the transfected neural tube (open square brackets).

studied how *ATF4* activates *Foxd3* transcription, and if *ATF4* is required for the initiation and/or maintenance of *Foxd3* expression. Nonetheless, *Foxd3* is probably one of the *ATF4* target genes in the neural crest EMT because the phenotype obtained by *ATF4* misexpression in the neural tube appears to be severer than that by *Foxd3* misexpression (compare studies by Dottori et al., 2001, Kos et al., 2001, and this study) and because the inhibition of EMT of BMP4-treated neural plate explants by *En-ATF4*$^{\Delta N}$ could not be rescued by cotransfection of *Foxd3* (YW, unpublished data). While the apicobasally polarized morphology of the neuroepithelial cells is maintained in the *Foxd3*-transfected neural tube, *ATF4*-transfected cells round up and fall off into the lumen of the neural tube. Such change in cell shape indicates cytoarchitectural modifications along with cell polarity loss and appears to be reminiscent of extensive cytoskeletal degradation and remodeling during EMT.

It has been known that, while *Foxd3* misexpression can induce HNK1 in the neural tube (Kos et al., 2001; Dottori et al., 2001), *ATF4* misexpression fails to do so. This can be explained, in part, by the fact that *Foxd3*, but not *ATF4*, can induce *Sox10* and that *Sox10*, in turn, can induce HNK1 (McKeown et al., 2005; Suzuki et al., 2006). Indeed, *ATF4* misexpression rather downregulates the basal expression of HNK1 epitope in the neural tube (see above). Therefore, *ATF4*-mediated downregulation of HNK1 expression should be attenuated in the crest cells. Because *Sox9* misexpression in the neural tube induces HNK1 no matter if *ATF4* is cotransfected, *Sox9* induction appears to be important for the successful expression of HNK1 in the neural crest.

Such complexity of the neural crest EMT regulatory network is also observed in the regulation of *Cadherin6B* expression. A previous report revealed that Snail2 represses *Cadherin6B* expression by a direct binding around its promoter region (Taneyhill et al. 2007). In this study, we show that *ATF4* represses *Cadherin6B* expression, probably by inducing *Foxd3*, without inducing *Snail2*. Thus, the tight regulation of *Cadherin6B* expression during the neural crest EMT is achieved by the combination of transcription factors' activities.

Stability control of ATF4 protein

While the importance of protein degradation/stability control in development has been increasingly recognized in recent years, there are only a few reports studying the role of protein degradation in neural crest formation (Voigt and Papalopulu, 2005; Vernon and LaBonne, 2006). For example, Cullin-1, the central scaffold component of SCF E3 ubiquitin ligase complex, is important for the allocation of neural crest domain in the ectoderm partly by degradating β-catenin in *Xenopus* embryos (Voigt and Papalopulu, 2005). Their results seem to be consistent with the fact that β-catenin is one of the target of SCF$^{\beta TrCP}$-mediated ubiquitination (Kitagawa et al., 1999). However, β-catenin is unlikely to be the only target for degradation because SCF complexes will ubiquitinate a wide range of proteins partly by using various F-box-containing subunits, which determine the target specificity. In fact, a previous report revealed that, in *Xenopus*, Ppa/Fbxl-14, an F-box-containing subunit, bound and ubiquitinated Snail2 to limit its expression level (Vernon and LaBonne, 2006). Except for these examples in *Xenopus*, little attention has been paid to the role of the regulation of protein stability in neural crest formation.

ATF4 has been known as an unstable protein, and serine phosphorylation of DSGICMS sequence in ATF4 by an unknown kinase promotes the binding of β-TrCP1 and subsequent ubiquitination and proteasomal degradation (Lassot et al., 2001). SCF$^{\beta\text{-}TrCP1}$–mediated degradation has been proposed as the mechanism to establish the tissue/cell type-restricted expression of ATF4 protein (Yang and Karsenty, 2004). Yet, it has been unclear how such degradation/stabilization is spatiotemporally controlled. As the expression of *β-TrCP1* and a related gene *β-TrCP2* has been shown to be regulated by Wnt signal in 293 T cells (Spiegelman et al., 2002), and canonical Wnt signaling is involved in neural crest induction and EMT promotion (García-Castro et al., 2002; Burstyn-Cohen et al., 2004; see also reviews mentioned above), it is reasonable to speculate that the crest specific stabilization of ATF4 protein may be mediated by the downregulation of *β-TrCP1/2* transcription. However, *β-TrCP1/2* expression does not seem to be regulated in a neural crest-specific manner (TS and YW, unpublished observation). Still, our mutation analysis of the β-TrCP binding site revealed an effective expression of ATF4 protein in the neural tube cells, suggesting that other mechanisms should contribute the neural crest-specific stabilization of ATF4 protein. In this study, we show that misexpression of *p300* in the neural tube increases the endogenous ATF4 protein expression. Our data not only uncover the importance of β-TrCP-mediated degradation to establish ATF4 expression specificity but also suggest the involvement of p300 in this process. Consistently, endogenous p300 protein level is remarkably high in pre-EMT crest cells, compared to the rest of the neural tube cells. Coincidently, both ATF4 and p300 proteins are highly expressed in the embryonic epidermal ectoderm (see above), while the role of these proteins there remains unknown. Yet, as *p300* mRNA is ubiquitously expressed, posttranscriptional regulation of *p300* expression in the neural crest formation will have to be examined in the future. Nonetheless, our current study emphasizes the importance of post-transcriptional regulation of gene expression in formation of the neural crest. Our inference in this study also well coincides with the recent findings uncovering the importance of posttranscriptional control of transcription factor expression in EMT, such as the degradation of Snail protein facilitated by GSK3-β signaling and SCF$^{\beta TrCP}$ function (Zhou et al., 2004) and the downregulation of *ZEB-1/ZEB-2* expression by a small noncoding RNA *miR200* (Park et al., 2008; Gregory et al., 2008; Korpal et al., 2008).

Acknowledgments

We thank Dr. Don Newgreen for comments on the manuscript. We are grateful to Dr. Daisuke Sakai for discussions. We thank Drs. C. Erickson, F. Gage, H. Nakamura, M. Uchikawa, S. Nakagawa, and M. Furuse for plasmids and an antibody. This work was supported in part by a grant to TS from Japan Science and Technology Agency (19. 55041).

Appendix A. Supplemental data

Supplementary data associated with this article can be found, in the online version, at doi:10.1016/j.ydbio.2010.05.492.

References

Acloque, H., Adams, M.S., Fishwick, K., Bronner-Fraser, M., Nieto, M.A., 2009. Epithelial–mesenchymal transitions: the importance of changing cell state in development and disease. J Clin. Invest. 119, 1438–1449.
Ameri, K., Harris, A.L., 2008. Activating transcription factor 4. Intl. J Biochem. Cell Biol. 40, 14–21.
Burstyn-Cohen, T., Stanleigh, J., Sela-Donenfeld, D., Kalcheim, C., 2004. Canonical Wnt activity regulates neural crest delamination linking BMP/Noggin signalling with G_1/S transition. Development 131, 5327–5339.
Cao, X., Pffaf, S.L., Gage, F.H., 2007. A functional study of miR-124 in the developing neural tube. Genes Dev. 21, 531–536.
Cheng, U., Cheung, M., Abu-Elmagd, M.M., Orme, A., Scotting, P.J., 2000. Chick sox10, a transcription factor expressed in both early neural crest cells and central nervous system. Brain Res. Dev. Brain Res. 121, 233–241.
Cheung, M., Briscoe, J., 2003. Neural crest development is regulated by the transcription factor Sox9. Development 130, 5681–5693.
Cheung, M., Chaboissier, M.C., Mynett, A., Hirst, E., Schedl, A., Briscoe, J., 2005. The transcriptional control of trunk neural crest induction, survival, and delamination. Dev. Cell 8, 179–192.
Cibeli, G., Schoch, S., Thiel, G., 1999. Nuclear targeting of cAMP response element binding proteins 2 (CREB2). Eur. J. Cell Biol. 78, 642–649.
Dottori, M., Gross, M.K., Labosky, P., Goulding, M., 2001. The winged-helix transcription factor Foxd3 suppresses interneuron differentiation and promotes neural crest cell fate. Development 128, 4127–4138.
Duband, J.L., Dufour, S., Yamada, S.S., Yamada, K.M., Thiery, J.P., 1991. Neural crest cell locomotion induced by antibodies to beta 1 integrins. A tool for studying the roles of substratum molecular avidity and density in migration. J. Cell Sci. 98, 517–532.
Endo, Y., Osumi, N., Wakamatsu, Y., 2002. Bimodal functions of Notch-mediated signaling are involved in neural crest formation during avian ectoderm development. Development 129, 863–873.
Endo, Y., Osumi, N., Wakamatsu, Y., 2003. Deltex/Dtx mediates NOTCH signaling in regulating Bmp4 expression for cranial neural crest formation during avian development. Dev. Growth Diff. 45, 241–248.
Funahashi, J., Okafuji, T., Ohuchi, H., Noji, S., Tanaka, H., Nakamura, H., 1999. Pax-5 regulates mid–hindbrain organizer's activity through an interaction with Fgf8. Dev. Growth Differ. 41, 59–72.
García-Castro, M., Marcelle, C., Bronner-Fraser, M., 2002. Ectodermal Wnt function as a neural crest inducer. Science 297, 848–851.
Gregory, P.A., Bert, A.G., Paterson, E.L., Barry, S.C., Tsykin, A., Farshid, G., Vadas, M.A., Khew-Goodall, Y., Goodall, G.J., 2008. The miR-200 family and miR-205 regulate epithelial to mesenchymal transition by targeting ZEB1 and SIP1. Nat. Cell Biol. 10, 593–601.
Hai, T., Hartman, M.G., 2001. The molecular biology and nomenclature of the activating transcription factor/cAMP responsive element binding family of transcription factors: activating transcription factor proteins and homeostasis. Gene 273, 1–11.
Hamburger, V., Hamilton, H.L., 1951. A series of normal stages in the development of the chick embryo. J. Morph. 88, 49–92.
Hettman, T., Barton, K., Leiden, J.M., 2000. Microphthalmia due to p53-mediated apoptosis of anterior lens epithelial cells in mice lacking the CREB-2 transcription factor. Dev. Biol. 222, 110–123.
Inoue, T., Nakamura, S., Osumi, N., 2000. Fate mapping of mouse prosencephalic neural plate. Dev. Biol. 219, 373–383.
Kalcheim, C., Burstyn-Cohen, T., 2005. Early stages of neural crest ontogeny: formation and regulation of cell delamination. Int. J. Dev. Biol. 49, 105–116.
Kalluri, R., Weeinberg, R.A., 2009. The basics of epithelial–mesenchymal transition. J Clin. Invest. 119, 1420–1428.
Kitagawa, M., Hatakeyama, S., Shirane, M., Matsumoto, M., Ishida, N., Hattori, K., Nakamichi, I., Kikuchi, A., Nakayama, K., Nakayama, K., 1999. An F-box protein, FWD1, mediates ubiquitin-dependent proteolysis of beta-catenin. EMBO J. 1, 2401–2410.
Kitajiri, S., Miyamoto, T., Mineharu, A., Sonoda, N., Furuse, K., Hata, M., Sasaki, H., Mori, Y., Kubota, T., Ito, J., Furuse, M., Tsukita, S., 2004. Compartmentalization established by claudin-11-based tight junctions in stria vascularis is required for hearing through generation of endocochlear potential. J. Cell Sci. 117, 5087–5096.
Korpal, M., Lee, E.S., Hu, G., Kang, Y., 2008. The miR-200 family inhibits epithelial–mesenchymal transition and cancer cell migration by direct targeting of E-cadherin transcriptional repressors ZEB1 and ZEB2. J. Biol. Chem. 283, 14910–14914.
Kos, R., Reedy, M.V., Johnson, R.L., Erickson, C.A., 2001. The winged-helix transcription factor FoxD3 is important for establishing the neural crest lineage and repressing melanogenesis in avian embryos. Development 128, 1467–1479.
Lassot, I., Segeral, E., Berlioz-Torrent, C., Durand, H., Groussin, L., Hai, T., Benarous, R., Margottin-Goguet, M., 2001. ATF4 degradation relies on a phosphorylation-dependent interaction with the SCF (betaTrCP) ubiquitin ligase. Mol. Cell. Biol. 21, 2192–2202.
Lassot, I., Estrabaud, E., Emiliani, S., Benkirane, M., Benarous, R., Margottin-Goguet, M., 2005. p300 modulates ATF4 stability and transcriptional activity independently of its acetyltransferase domain. J. Biol. Chem. 280, 41537–41545.
Le Douarin, N.M., Kalcheim, C., 1999. The Neural Crest 2nd edition. Cambridge University Press, Cambridge.
Masuoka, H.C., Townes, T.M., 2002. Targeted disruption of the activating transcription factor 4 gene results in severe fetal anemia in mice. Blood 99, 736–745.
Matsunaga, E., Araki, I., Nakamura, H., 2000. Pax6 defines the di-mesencephalic boundary by repressing En1 and Pax2. Development 127, 2357–2365.
Matsumata, M., Uchikawa, M., Kamachi, Y., Kondoh, H., 2005. Multiple N-cadherin enhancers identified by systematic functional screening indicate its Group B1 SOX-dependent regulation in neural and placodal development. Dev. Biol. 286, 601–617.
McKeown, S.J., Lee, V.M., Bronner-Fraser, M., Newgreen, D.F., Farlie, P.G., 2005. Sox10 overexpression induces neural crest-like cells from all dorsoventral levels of the neural tube but inhibits differentiation. Dev. Dyn. 233, 430–444.
Murphy, P., Kolstø, A., 2000. Expression of the bZIP transcription factor TCF11 and its potential dimerization partners during development. Mech. Dev. 97, 141–148.
Nakagawa, S., Takeichi, M., 1995. Neural crest cell–cell adhesion controlled by sequential and subpopulation specific expression of novel cadherins. Development 121, 1321–1332.
Neito, M.A., Sargent, M.G., Wilkinson, D.G., Cooke, J., 1994. Control of cell behavior during vertebrate development by Slug, a zinc finger gene. Science 264, 835–839.
Park, S.M., Gaur, A.B., Lengyel, E., Peter, M.E., 2008. The miR-200 family determines the epithelial phenotype of cancer cells by targeting the E-cadherin repressors ZEB1 and ZEB2. Genes Dev. 22, 894–907.
Sakai, D., Tanaka, Y., Endo, Y., Osumi, N., Okamoto, H., Wakamatsu, Y., 2005. Regulation of Slug transcription in embryonic ectoderm by beta-catenin-Lef/Tcf and BMP-Smad signaling. Dev. Growth Differ. 47, 471–482.
Sakai, D., Wakamatsu, Y., 2005. Regulatory mechanisms for neural crest formation. Cells Tissues Organs 179, 24–35.
Sakai, D., Suzuki, T., Osumi, N., Wakamatsu, Y., 2006. Cooperative action of Sox9, Snail2, and PKA signaling in early neural crest development. Development 133, 1323–1333.
Sauka-Spengler, T., Bronner-Fraser, M., 2008. A gene regulatory network orchestrates neural crest formation. Nat. Rev. Mol. Cell Biol. 9, 557–568.
Schoch, S., Cibelli, G., Magin, A., Steinmüller, L., Thiel, G., 2001. Modular structure of cAMP response element binding protein 2 (CREB2). Neurochem. Int. 38, 601–608.
Spiegelman, V.S., Tang, W., Katoh, M., Slaga, T.J., Fuchs, S.Y., 2002. Inhibition of HOS expression and activities by Wnt pathway. Oncogene 21, 856–860.
Suzuki, T., Sakai, D., Osumi, N., Wada, H., Wakamatsu, Y., 2006. Sox genes regulate type 2 collagen expression in avian neural crest cells. Dev. Growth Differ. 48, 477–486.
Tanaka, T., Tsujimura, T., Takeda, K., Sugihara, A., Maekawa, A., Terada, N., Yoshida, N., Akira, S., 1998. Targeted disruption of ATF4 discloses its essential role in the formation of eye lens fibres. Genes Cells 3, 801–810.
Taneyhill, L.A., Coles, E.G., Bronner-Fraser, M., 2007. Snail2 directly represses cadherin6B during epithelial-to-mesenchymal transitions of the neural crest. Development 134, 1481–1490.
Taylor, K.M., LaBonne, C., 2006. SoxE factors function equivalently during neural crest and inner ear development and their activity is regulated by SUMOylation. Develop. Cell 9, 593–603.
Tucker, G.C., Delarue, M., Zada, S., Boucaut, J.C., Thiery, J.P., 1988. Expression of the HNK-1/NC-1 epitope in early vertebrate neurogenesis. Cell Tissue Res. 251, 457–465.
Vernon, A.E., LaBonne, C., 2006. Slug stability is dynamically regulated during neural crest development by the F-box protein Ppa. Development 133, 3359–3370.
Voigt, J., Papalopulu, N., 2005. A dominant-negative form of the E3 ubiquitin ligase Cullin-1 disrupts the correct allocation of cell fate in the neural crest lineage. Development 133, 559–568.
Wakamatsu, Y., Watanabe, Y., Shimono, A., Kondoh, H., 1993. Transition of localization of the N-myc protein from nucleus to cytoplasm in differentiating neurons. Neuron 10, 1–9.
Wakamatsu, Y., Watanabe, Y., Nakamura, H., Kondoh, H., 1997. Regulation of the neural crest cell fate by N-myc: promotion of ventral migration and neuronal differentiation. Development 124, 1953–1962.
Wakamatsu, Y., Weston, J.A., 1997. Sequential expression and role of Hu RNA-binding proteins during neurogenesis. Development 124, 3449–3460.
Wakamatsu, Y., Endo, Y., Osumi, N., Weston, J.A., 2004. Multiple roles of SOX2, a HMG-box transcription factor in avian development. Dev. Dyn. 229, 74–86.
Yang, X., Karsenty, G., 2004. ATF4, the osteoblast accumulation of which is determined post-translationally, can induce osteoblast-specific gene expression in non-osteoblastic cells. J. Biol. Chem. 279, 47109–47114.
Zhou, B.P., Deng, J., Xia, W., Xu, J., Li, Y.M., Gunduz, M., Hung, M.-C., 2004. Dual regulation of Snail by GSK-3b-mediated phosphorylation in control of epithelial-mesenchymal transition. Nat. Cell Biol. 6, 931–940.